IEEE Access
Multidisciplinary | Rapid Review | Open Access Journal

Received 12 January 2024, accepted 22 January 2024, date of publication 24 January 2024, date of current version 15 February 2024.

Digital Object Identifier 10.1109/ACCESS.2024.3357989

RESEARCH ARTICLE

Improved Coyote Optimization Algorithm and Deep Learning Driven Activity Recognition in Healthcare

SANA ALAZWARI[1], MAJDY M. ELTAHIR[2], NABIL SHARAF ALMALKI[3], ABDULRAHMAN ALZAHRANI[4], MRIM M. ALNFIAI[1], AND AHMED S. SALAMA[5]

[1]Department of Information Technology, College of Computers and Information Technology, Taif University, Taif 21944, Saudi Arabia
[2]Department of Information Systems, College of Science and Art at Mahayil, King Khalid University, Abha 61421, Saudi Arabia
[3]Department of Special Education, College of Education, King Saud University, Riyadh 12372, Saudi Arabia
[4]Department of Computer Science and Engineering, College of Computer Science and Engineering, University of Hafr Al Batin, Hafar Al Batin 39524, Saudi Arabia
[5]Department of Electrical Engineering, Faculty of Engineering and Technology, Future University in Egypt, New Cairo 11845, Egypt

Corresponding author: Mrim M. Alnfiai (m.alnofiee@tu.edu.sa)

The authors extend their appreciation to the Deanship of Scientific Research at King Khalid University for funding this work through large group Research Project under grant number (RGP2/29/44). Research Supporting Project number (RSPD2024R521), King Saud University, Riyadh, Saudi Arabia. This study is partially funded by the Future University in Egypt (FUE).

ABSTRACT Healthcare is an area of concern where the application of human-centred design practices and principles can enormously affect well-being and patient care. The provision of high-quality healthcare services requires a deep understanding of patients' needs, experiences, and preferences. Human activity recognition (HAR) is paramount in healthcare monitoring by using machine learning (ML), sensor data, and artificial intelligence (AI) to track and discern individuals' behaviours and physical movements. This technology allows healthcare professionals to remotely monitor patients, thereby ensuring they adhere to prescribed rehabilitation or exercise routines, and identify falls or anomalies, improving overall care and safety of the patient. HAR for healthcare monitoring, driven by deep learning (DL) algorithms, leverages neural networks and large quantities of sensor information to autonomously and accurately detect and track patients' behaviors and physical activities. DL-based HAR provides a cutting-edge solution for healthcare professionals to provide precise and more proactive interventions, reducing the burden on healthcare systems and improving patient well-being while increasing the overall quality of care. Therefore, the study presents an improved coyote optimization algorithm with a deep learning-assisted HAR (ICOADL-HAR) approach for healthcare monitoring. The purpose of the ICOADL-HAR technique is to analyze the sensor information of the patients to determine the different kinds of activities. In the primary stage, the ICOADL-HAR model allows a data normalization process using the Z-score approach. For activity recognition, the ICOADL-HAR technique employs an attention-based long short-term memory (ALSTM) model. Finally, the hyperparameter tuning of the ALSTM model can be performed by using ICOA. The stimulation validation of the ICOADL-HAR model takes place using benchmark HAR datasets. The wide-ranging comparison analysis highlighted the improved recognition rate of the ICOADL-HAR method compared to other existing HAR approaches in terms of various measures.

INDEX TERMS Human activity recognition, hyperparameter tuning, coyote optimization algorithm, wearable sensor, deep learning.

I. INTRODUCTION

Generally, hospitalized patients spend their time mostly in bed and become lazy. It is particularly for elder patients as physically inactive where hospitalization leads to useful

The associate editor coordinating the review of this manuscript and approving it for publication was Sotirios Goudos.

decay [1]. In addition, better or steady action stages aid as a valued effort for evaluating patient's discharge willingness. In the present scenario, observing hospitalized patient's flexibility depends mainly on direct opinions from caregivers [2]. Multiple tools are accessible to evaluate the functional and mobility capability of patients. A selection of which valuation tool to utilize mainly relies on feasibility and the clinician's choice. Wearable accelerometers have a high possibility to perform as an effective tool in estimating patients' health condition at the time of recovery in a neutral method and allowing assessment of analysis and other medicinal interventions [3]. Metrics like the quantity of time consumed in a decent place as well as regular step count initiate have a good relation with the period of hospital stay. Additionally, posture detection models deliver significant data for averting pressure ulcer creation [4]. These metrics defined by employing human activity recognition (HAR) depend on wearable sensors or camera methods like gyroscopes, magnetometers accelerometers as well as barometric pressure devices. Handling indications from wearable devices needs much computation control when equated to camera-related methods as well as executing a few assaults of confidentiality [5]. HAR employs accelerometers in smartphones and smartwatches as fitness trackers.

HAR contains dual kinds of actions such as complex and simple [6]. Complex human actions include the execution of simple human movements along with exact transition acts, there are moderately few studies on recognizing difficult human actions like dribbling a ball, brushing teeth, and so on. In the machine learning (ML) field, HAR employs labelled data because it is a multivariate time series detection as well as a supervised learning issue [7]. HAR is mainly attained by removing physically crafted features from device data as well as training classifiers that learn relationships and patterns among features as well as class labels. It is nothing but a conventional technique that uses feature-based ML models. Many past researchers discovered the task of detection activity by utilizing traditional techniques like Random Forest, SVM, XGBoost, etc. as well as non-traditional deep learning (DL) methods [8]. The task with traditional methods needed a lot of feature engineering as well as physical feature extraction which is time-consuming. Recently, deep neural networks (DNNs) are an effective method which becomes a general and another method selection for HAR [9]. DNNs were proposed and innovative in present years and brought innovations in areas like natural language processing and visual object detection. The main benefit of employing DNNs is that conventional ML models are capable of removing higher-level features mechanically from raw input so that hand-crafted feature extraction is not needed [10]. DL models automatically learn features from data and are more appropriate for the task of classifying difficult human actions.

This study presents an improved coyote optimization algorithm with a deep learning-assisted HAR (ICOADL-HAR) approach for healthcare monitoring. The purpose of the ICOADL-HAR technique is to analyze the sensor information of the patients to determine the different types of activities. In the primary stage, the ICOADL-HAR model allows a data normalization process using the Z-score approach. For activity recognition, the ICOADL-HAR technique employs an attention-based long short-term memory (ALSTM) network. Finally, the hyperparameter tuning of the ALSTM algorithm can be performed by using the ICOA. The design of the ICOA for hyperparameter tuning demonstrates the novelty of the work. The stimulation validation of the ICOADL-HAR method takes place using benchmark HAR datasets.

II. LITERATURE SURVEY

In [11], a HAR transfer-learning model with two major mechanisms was introduced. Firstly, a representative analysis shows general characteristics that are transmitted through user-specific features and users should be personalized. In [12], the authors suggest a hierarchical DL-based HAR model (HiHAR) to augment the short, long -term and spatial features from the sensor information which is built from two robust DNN structures: Bi-LSTM and CNN. HiHAR has two phases with the hierarchical architecture: local and global. In [13], the authors carried out smartphone sensor-based raw data collections, such as H-Activity, using Android-OS-based applications for linear acceleration, gyroscope, and accelerometer. Moreover, a hybrid DL algorithm is introduced, coupling CNN-LSTM, enabled by the self-attention mechanism to improve the predictive abilities of the model. In [14], proposed a new classifier ''ICGNet'' for HAR that is a mixture of GRU and CNN models. In this work, the CNN block used is adapted from the Inception model. Simultaneously, it exploits multi-sized convolution filters over the input thereby capturing the data at various scales.

In [15], to support an IoT system that requires a resource-effective mechanism, the study presents a DL-based HAR technique named MultiCNN-FilterLSTM that fuses a multi-head CNN with LSTM via residual connection where the feature vector is processed efficiently in hierarchical order. In [16], a wearable inertial measurement unit system to assess patients through the Berg balance scale (BBS), a clinical test for balance assessment. An automated scoring model was introduced for these purposes. The study aims to enhance the accuracy of ML-based techniques by presenting a DL model. A 1D-CNN and GRU that show better accuracy in multi-variate time-series data are applied to find the optimum ensemble model. We tested different structures, and a stacked ensemble mechanism with a meta-learner after one GRU head and two 1D-CNN heads revealed higher performance.

In [17], the authors focus on reinforcing the vanilla convolution without modifying the model architecture in HAR scenarios. We introduce a new heterogeneous convolution for the HAR task based on the concept of grouped convolution, where each filter within a certain convolution layer is divided into two unequal groups. Especially, the sensor inputs are down-sampled into low-dimension embedding that is

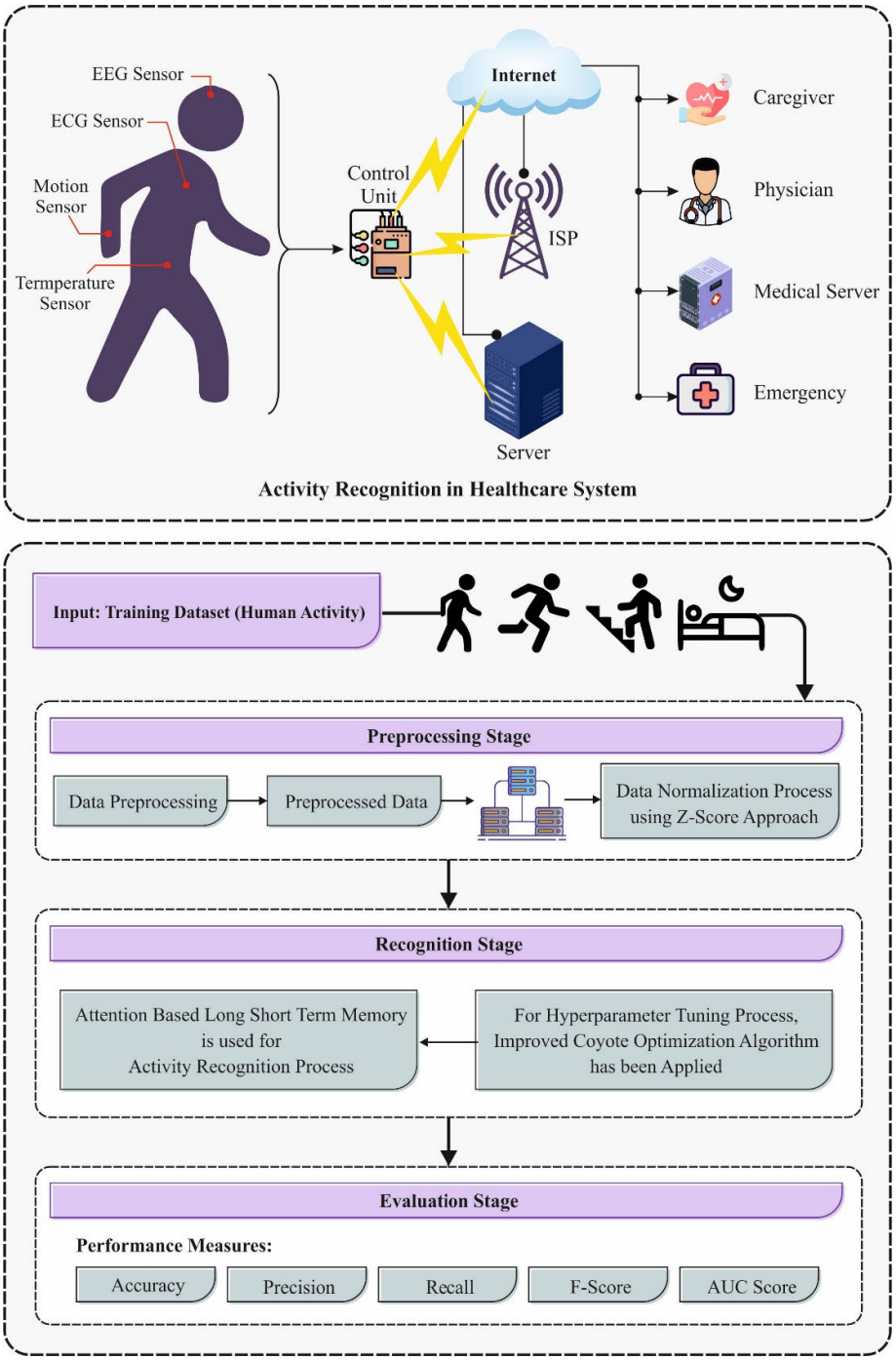

FIGURE 1. Overall flow of ICOADL-HAR technique.

convolved via single filter groups to rectify the standard filter within the other groups.

Abdulelah et al. [18] introduce a HAR lightweight, lower computational ability, DL algorithm for real-time application. The general HAR architecture for smartphone sensor information is developed by using the LSTM network for the time-series domain and typical CNN exploited for classification. The finding demonstrates that the presented technique surpasses many of the deployed DL and ML algorithms.

III. THE PROPOSED METHOD

In this study, we have established an ICOADL-HAR approach for healthcare monitoring. The purpose of the ICOADL-HAR technique is to analyze the sensor information of the patients to determine the different kinds

of activities. It contains three main processes such as Z-score normalization, ALSTM-based classification, and ICOA-based hyperparameter tuning. The overall working flow of the ICOADL-HAR model is given in Fig. 1.

A. DATA NORMALIZATION

Initially, the ICOADL-HAR algorithm allows a data normalization process using the Z-score technique. Z-score normalization is a central data preprocessing model in HAR that ensures the comparability of sensor information gathered from various individuals or devices [19]. Z-score normalization alleviates the effects of variations in sensor units and sensitivity by converting raw sensor measurements into a normalized scale with a mean of zero and a standard deviation of one, which makes it easy to analyze and identify patterns of human activities across different subjects and equipment. This normalization technique optimizes the accuracy of the HAR model and simplifies the incorporation of data from various sources, which contributes towards more reliable and robust activity recognition and healthcare monitoring systems.

B. ACTIVITY RECOGNITION IN THE CLASSIFICATION MODEL

At this stage, the ICOADL-HAR technique employs the ALSTM model. LSTM donates a difference in recurrent neural networks (RNNs) design [20]. One of the foremost benefits of this kind is the capability to absorb long-term needs. By consuming this technique, the LSTM system design accounts for faults existing in normal RNN like vanishing gradients. A simple LSTM network contains 3 fundamental measures including hidden layer (HL), input, and output layers. Several neurons in the input layer are verbalized through the quantity of features. Similarly, the output layer is based on the amount of objective features. This makes it an essential model to handle multivariate prediction. The uniqueness of LSTM relies on the usage of memory units within HL. This includes 3 kinds of gates namely forget f_t, input i_t, and output 0_t, whereas t represents timestep. Particular gates are employed by memory cells to modify cell states s_t, well permitting data to be kept within the system. This device permits LSTM networks to make time-based alterations in data which makes them suitable to time-series information. Numerous phases are occupied within the LSTM network for each timestep t which are mentioned below:

Step 1: Data in cell state s_{t-1} measured for removal. Inputs are handled through the sigmoid activation function as well as predictable to a range of [0, 1], and then data is nominated for preservation from the preceding cell state or removal. The f_t forget gate is defined in Eq. (1):

$$f_t = \sigma\left(W_{f,x}x_t + W_{f,h}h_{t-1} + b_f\right) \tag{1}$$

whereas σ signifies the sigmoid function, $W_{f,x}$, and $W_{f,h}$ indicates weight matrices, x_t denoted as an input vector at timestep t, the output of preceding timestep $(t-1)$ signified by $h+t-1$ and b_f denotes forget gate bias vector.

Step 2: Inputs calculated and based on it data is enlarged to cell state s_t by utilizing a sigmoid function. Additionally, input data is proposed to a $[-1, 1]$ array through *thetanh* function. Two parameters are required to be calculated in this phase, activation values and candidate values for every input gate. These are expressed by employing Eqs. (2) and (3) correspondingly.

$$\tilde{s} = \tanh\left(W_{\tilde{s},x}x_t + W_{\tilde{s},h}x_t + b_{\tilde{s}}\right) \tag{2}$$

$$i_t = \tanh\left(W_{i,x}x_t + W_{i,h}x_t + b_i\right) \tag{3}$$

where bias vectors are characterized as $b_{\tilde{s}}$ and $b_{\tilde{i}}$, and weight matrices are denoted by $W_{\tilde{s},x}x_t$, $W_{\tilde{s},h}$, $W_{i,x}x_t$, $W_{i,h}x_t$.

Step 3: Novel cell states s_t are calculated depending on Eq. (4)

$$s_t = f_t \circ s_{t-1} + i_t \circ \tilde{s} \tag{4}$$

While symbol $(\circ)$ represents Hadamard product.

Step 4: Outputs of h_t defined through sigmoid and *tanh* activation functions calculated based on Eqs. (5) and (6) separately,

$$o_t = \sigma\left(W_{o,x}x_t + W_{o,h}h_{t-1} + b_{\mathrm{o}}\right) \tag{5}$$

$$h_t = \mathrm{o}_t \circ tanh\left(\mathrm{s_t}\right) \tag{6}$$

whereas σ signifies the sigmoid function, $W_{\mathrm{o},h}$, and $W_{o,x}$ characterize weight matrices and b_{o} is denoted by the bias vector.

By integrating these devices, an LSTM network can achieve the effect of short-term memory, via the implementation of 3 gates [21]. Moreover, cell memory permits preceding steps to impact future consequences that make LSTM networks more suitable for HAR. In HAR problems, the input feature is not of equal importance under various circumstances, we add the attention module to attain relevant data from significant features. The structure of the ALSTM model is shown in Fig. 2. Consider that Y is comprised of output $[y_{t-1}, y_t, y_{t+1}, \ldots]$ of the prior layer and the scoring model is implemented by the output score α and *Softmax* layer. Finally, Y is denoted as $\gamma.\gamma$ is comprised of weighted sum of $[y_{t-1}, y_t, y_{t+1}, \ldots]$:

$$M = \tanh\left(Y\right) \tag{7}$$

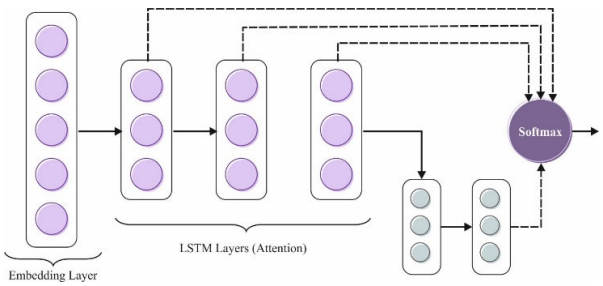

FIGURE 2. Architecture of ALSTM.

$$\alpha = soft\max\left(w^T M\right) \tag{8}$$

$$\gamma / = Y\alpha^T \tag{9}$$

where $Y \in R^{\mu\times\tau}$, μ denotes the dimension of the intention feature, w^T represents the transposition of w, w shows the training parameter, and τ indicates the dimension of time-sequence data. Lastly, the intention expression y' is attained by the tanh function.

$$y' = \tanh(\gamma) \tag{10}$$

C. ICOA-BASED HYPERPARAMETER TUNING

Finally, the hyperparameter tuning of the ALSTM model can be performed by the use of the ICOA. ICOA is a bio-inspired process of optimizer [22]. Similar to other nature-inspired techniques, nature has been simulated to solve the optimizer problems. COA mimics the living style of Coyotes which are Canis Latrans creatures existing mostly in Central and North America. The variation of the coyote to the environment and the coyote's social attitude has been exposed by the COA. The COA offers the procedure of optimizer using strike a balance between development and finding.

In the COA, the swarm has been separated as N_P sets where N_c defines the coyotes' number from all the sets. The candidate's performances and social attitude toward coyotes (SAC) are the main functions:

$$SAC_c^{g,t} = y = [y_1, y_2, \ldots, y_D] \tag{11}$$

At this point, $SAC_c^{g,t}$ defines the social attitude of c^{th} coyote from the g^{th} set at the simulation time of t.

Any coyotes are elected on an arbitrary basis to create the candidate solutions with the area performance.

$$SAC_{c,j}^{g,t} = LB_j + k \times \left(Hr_j - Lr_j\right) \tag{12}$$

whereas, k refers to the arbitrary amount different from 0 to 1, Hr_j and Lr_j imply the higher and lower ranges of the j^{th} variable throughout the seeking region. The cost function for all the coyotes has been considered using the below equation:

$$obj_c^{g,t} = f\left(SAC_{c,j}^{g,t}\right) \tag{13}$$

At the COA commencement, all the Coyotes participate from sets arbitrarily. All the individuals, also, variations the condition using moving to the other sets.

$$P_l = \frac{5}{100} \times N_c^2 \tag{14}$$

This equation does support altering the procedure of coyotes in all the sets. Not all the sets have 14 or more coyotes due to the enhanced diversity of COA. It is crucial to notice that whenever $Nc \leq 10\sqrt{2}$, P_1 develops superior to one.

The coyote leader from all the sets is called Alpha Coyote who is well known for the presence of a great responsible coyote. This equation below is employed for the detection of Alpha coyotes because of mathematics:

$$\alpha_c^{g,t} = sac_c^{g,t} forminob^{g,t} j_c \tag{15}$$

This mathematical equation below can depict the coyote's normal features for the interchange of culture:

$$cul_j^{g,t} = \begin{cases} R^{g,t}_{\frac{N_C+1}{2},j}, & N_c \text{ is an odd number} \\ \frac{1}{2}\left(R^{g,t}_{\frac{N_C}{2},j} + R^{g,t}_{\frac{N_C+1}{2},j}\right) & O.W. \end{cases} \tag{16}$$

where $R^{g,t}$ defines the social ranking for the set number (g) at t is a time interval for *the* j^{th} variable.

The life process of coyotes, an environmental element group, and the social attitude are also regarded by the COA. The coyote's life process is exposed depending on the equation:

$$Ble_j^{g,t} = \begin{cases} sac^{g,t}_{k_1,j}, & k_j < gk_s orj = j_1 \\ sac^{g,t}_{k_2,j}, & k_j \geq gk_s + gk_a orj = j_2 \\ \rho_j, & O.W. \end{cases} \tag{17}$$

At this point, k_i refers to the random number differing from 0 to 1, k2 indicates the arbitrary coyote from the g^{th} set, ρ_i demonstrates the arbitrarily selected number from the range of the designed variable, j_1, and j_2 illustrates the arbitrarily designed variables, gk_a and gk_s signifies the scatter and association chances that expose the cultural variation of coyotes in the set. The final elements are mathematical models are determined as follows:

$$gk_s = \frac{1}{d} \tag{18}$$

$$gk_a = \frac{1}{2}(1 - gk_s) \tag{19}$$

At present, d represents the dimensional of a variable.

The death possibility for *Ble* is considered 10 percent, i exposes the coyote counts from every set, and ω refers to the worse performances of coyotes.

The replacement of culture among sets is determined using μ_1 and μ_2 as:

$$\mu_1 = \alpha_c^{g,t} - sac_{c1}^{g_i t} \tag{20}$$

$$\mu_2 = cul^{g,t} - sac_{c2}^{g,t} \tag{21}$$

Now, the cultural dissimilarity among the elected coyotes (c1 and c2) and the group leader is signified by μ_1 and μ_2, correspondingly.

This equation below is employed to renew the social style because of the effect of the sets and the leader together:

$$nsac_c^{g,t} = sac_c^{g,t} + k_1 \times \mu_1 + k_2 \times \mu_2 \tag{22}$$

At this point, k_1 and k_2 indicate the random numbers among 0 and 1.

According to the renewing equation, this formula below offers the upgraded count of cost function as:

$$nobj_c^{g,t} = f\left(nsac_c^{g,t}\right) \tag{23}$$

$$sac_c^{g,t+1} = \begin{cases} nsac_c^{g,t}, & nobj_c^{g,t} < obj_c^{g,t} \\ sac_c^{g,t}, & O.W. \end{cases} \tag{24}$$

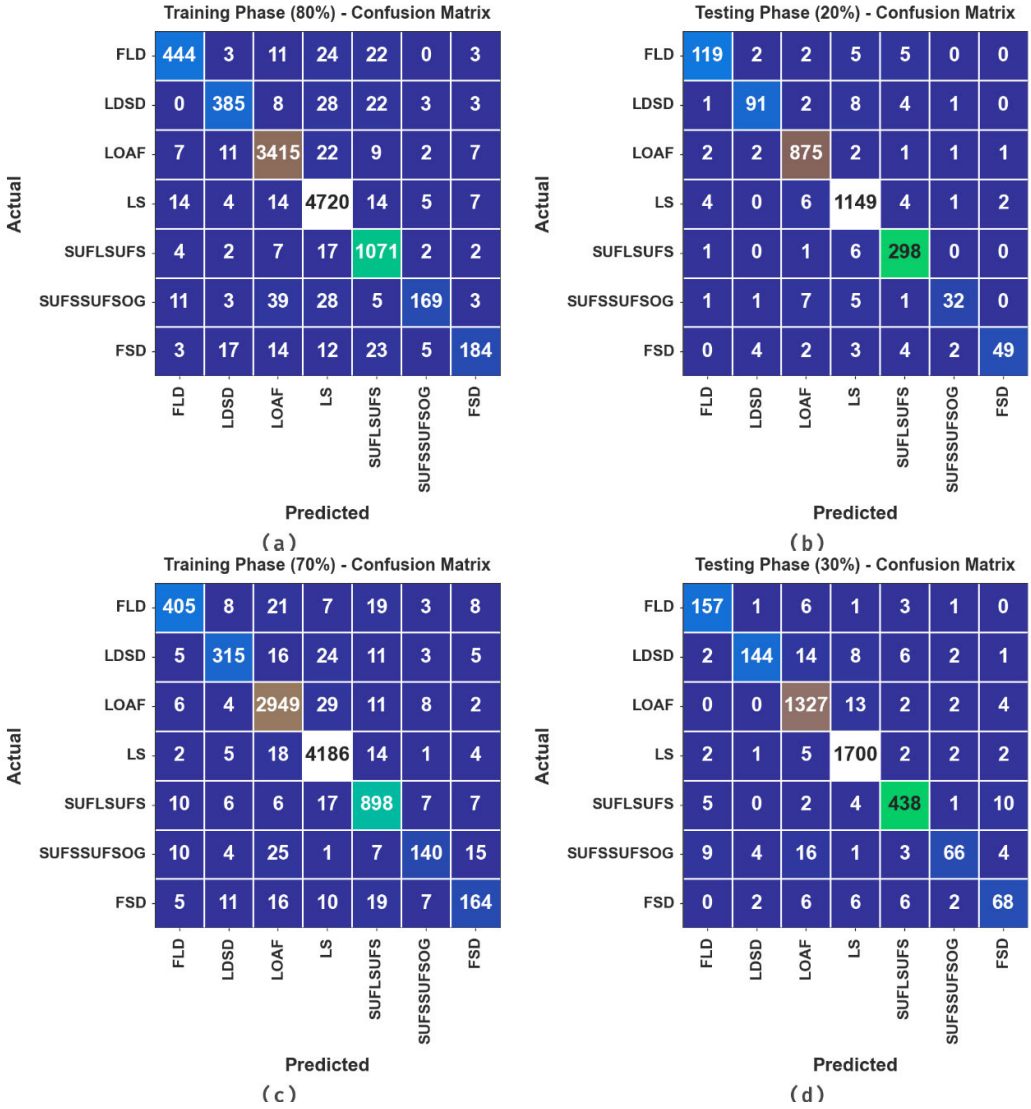

FIGURE 3. Confusion matrices of (a-b) 80:20 of TRPH/TSPH and (c-d) 70:30 of TRPH/TSPH.

A particular one main feature of this method is its capability not to be stuck from a local optimal. The ICOA technique derives an FF to obtain a higher efficacy of classification. It defines a positive integer to illustrate the best results of the candidate solution. At this point, the decline of the classifier error rate is assumed as an FF.

$$fitness\,(x_i) = Classifier\ Error\ Rate\,(x_i) = \frac{No.of\ misclassified\ samples}{Total\ No.of\ samples} * 100 \quad (25)$$

IV. EXPERIMENTAL VALIDATION

The simulation analysis of the ICOADL-HAR model was conducted on Localization Data for Person Activity (LDPA) datasets retrieved from the UCI dataset.

It includes seven classes such as LDSD (Lying down, sitting down), FLD (Falling, lying down), LS (Lying, sitting), LOAF (Lying, on all fours), SUFSSUFSOG (Standing up from sitting, standing up from sitting on the ground), FSD (Falling, sitting down) and SUFLSUFS (Standing up from lying, standing up from sitting) as shown in Table 1.

TABLE 1. Details on databases.

No. of classes	No. of Samples
FLD	640
LDSD	556
LOAF	4357
LS	5944
SUFLSUFS	1411
SUFSSUFSOG	305
FSD	322
Total Samples	13535

In Fig. 3, the confusion matrices produced by the AOAFS-HDLCP technique under 80:20 and 70:30 of the TR set/TS set are depicted. The results indicate the effectual detection and classification of seven classes.

In Table 2 and Fig. 4, the overall HAR outcomes of the ICOADL-HAR model are investigated under 80:20 of TRPH/TSPH. The outcomes imply that the ICOADL-HAR model properly recognizes human activities. On 80% of TRPH, the ICOADL-HAR technique offers an average $accu_y$ of 98.84%, $prec_n$ of 92.56%, $reca_l$ of 86.31%, F_{score} of 88.99%, and AUC_{score} of 92.76%. Meanwhile, on 20% of TSPH, the ICOADL-HAR method offers an average $accu_y$ of 99.01%, $prec_n$ of 93.43%, $reca_l$ of 87.73%, F_{score} of 90.27%, and AUC_{score} of 93.52%.

TABLE 2. HAR outcome of ICOADL-HAR technique on 80:20 of TRPH/TSPH.

Classes	$Accu_y$	$Prec_n$	$Reca_l$	F_{Score}	AUC_{Score}
Training Phase (80%)					
FLD	99.06	91.93	87.57	89.70	93.60
LDSD	99.04	90.59	85.75	88.10	92.68
LOAF	98.61	97.35	98.33	97.84	98.53
LS	98.25	97.30	98.79	98.04	98.31
SUFLSUFS	98.81	91.85	96.92	94.32	97.97
SUFSSUFSOG	99.02	90.86	65.50	76.13	82.67
FSD	99.09	88.04	71.32	78.80	85.54
Average	98.84	92.56	86.31	88.99	92.76
Testing Phase (20%)					
FLD	99.15	92.97	89.47	91.19	94.56
LDSD	99.08	91.00	85.05	87.92	92.35
LOAF	98.93	97.77	98.98	98.37	98.94
LS	98.30	97.54	98.54	98.04	98.33
SUFLSUFS	99.00	94.01	97.39	95.67	98.30
SUFSSUFSOG	99.26	86.49	68.09	76.19	83.95
FSD	99.34	94.23	76.56	84.48	88.22
Average	99.01	93.43	87.73	90.27	93.52

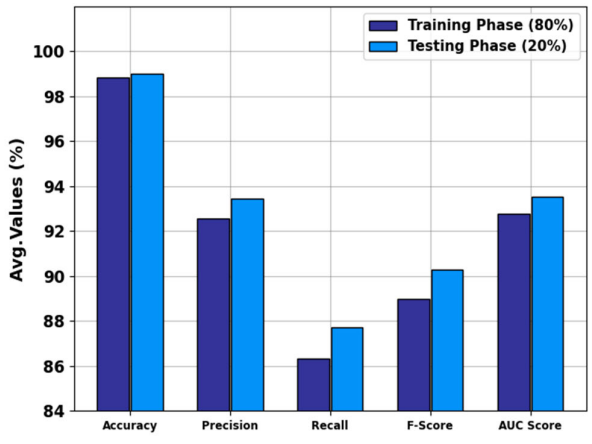

FIGURE 4. Average of ICOADL-HAR technique on 80:20 of TRPH/TSPH.

In Table 3 and Fig. 5, the overall HAR outcomes of the ICOADL-HAR method are investigated under 70:30 of TRPH/TSPH. The outcomes imply that the ICOADL-HAR model properly recognizes human activities. On 70% of TRPH, the ICOADL-HAR method provides an average $accu_y$ of 98.74%, $prec_n$ of 89.97%, $reca_l$ of 85.78%, F_{score} of 87.72%, and AUC_{score} of 92.48%. Meanwhile, on 30% of TSPH, the ICOADL-HAR method offers an average $accu_y$ of 98.87%, $prec_n$ of 91.06%, $reca_l$ of 86.68%, F_{score} of 88.55%, and AUC_{score} of 92.96%.

TABLE 3. HAR outcome of ICOADL-HAR technique on 70:30 of TRPH/TSPH.

Classes	$Accu_y$	$Prec_n$	$Reca_l$	F_{Score}	AUC_{Score}
Training Phase (70%)					
FLD	98.90	91.42	85.99	88.62	92.78
LDSD	98.92	89.24	83.11	86.07	91.35
LOAF	98.29	96.66	98.01	97.33	98.21
LS	98.61	97.94	98.96	98.45	98.64
SUFLSUFS	98.59	91.73	94.43	93.06	96.74
SUFSSUFSOG	99.04	82.84	69.31	75.47	84.50
FSD	98.85	80.00	70.69	75.06	85.12
Average	98.74	89.97	85.78	87.72	92.48
Testing Phase (30%)					
FLD	99.26	89.71	92.90	91.28	96.22
LDSD	98.99	94.74	81.36	87.54	90.57
LOAF	98.28	96.44	98.44	97.43	98.32
LS	98.84	98.10	99.18	98.64	98.89
SUFLSUFS	98.92	95.22	95.22	95.22	97.30
SUFSSUFSOG	98.84	86.84	64.08	73.74	81.91
FSD	98.94	76.40	75.56	75.98	87.51
Average	98.87	91.06	86.68	88.55	92.96

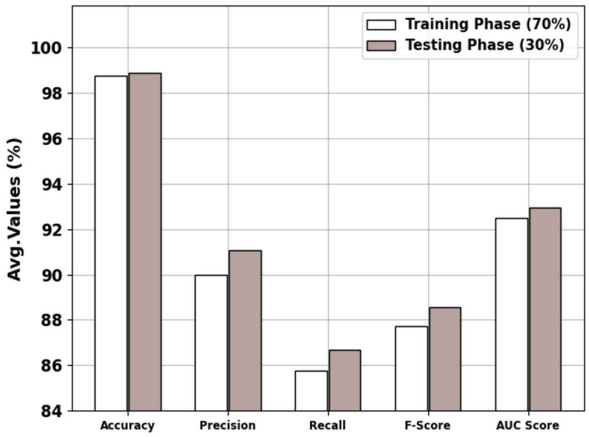

FIGURE 5. Average of ICOADL-HAR method on 70:30 of TRPH/TSPH.

The training and validation accuracy curves of the ICOADL-HAR technique on 80:20 of TRPH/TSPH shown in Fig. 6, provide valuable insights into the performance of the ICOADL-HAR technique over multiple epochs. This curve highlights the valuable insights into the learning process and the model's capacity to generalize. Furthermore, it is noted that there is a consistency improvement in the TR and TS accuracy over maximum epochs. It noted that the model's capacity to learn and detect patterns within the training and testing datasets. The increasing testing accuracy proposes that the model adapts to the training dataset and excels in making accurate predictions on previously unseen data, which emphasizes the strong generalization abilities.

In Fig. 7, we represent a comprehensive view of the TR and TS loss values for the ICOADL-HAR technique on 80:20 of TRPH/TSPH across various epochs. The TR loss progressively decreases as the model enhances its weights to reduce classifier errors on TR and TS datasets.

This loss curve provides a better understanding of how well the model aligns with the training data, underlining its capability to efficiently hold patterns in both datasets. It is noticeable that the ICOADL-HAR method incessantly refines

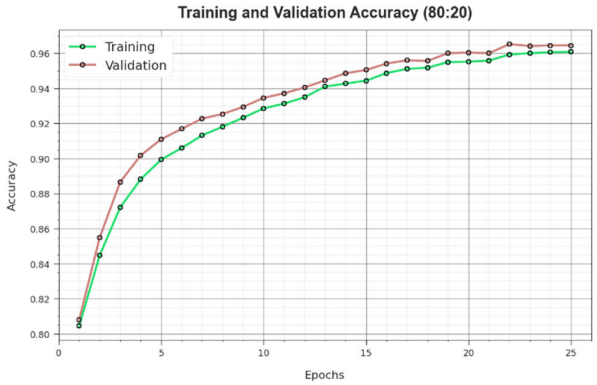

FIGURE 6. *Accu$_y$* curve of ICOADL-HAR technique on 80:20 of TRPH/TSPH.

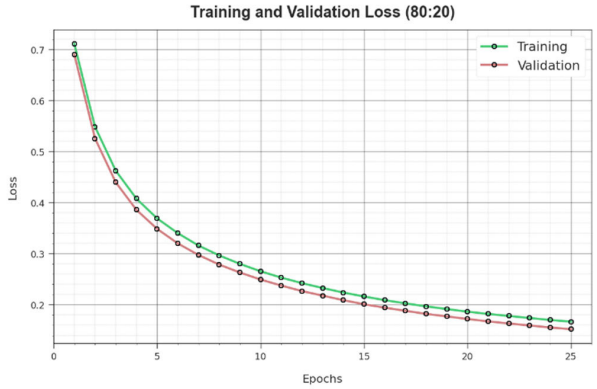

FIGURE 7. Loss curve of ICOADL-HAR technique on 80:20 of TRPH/TSPH.

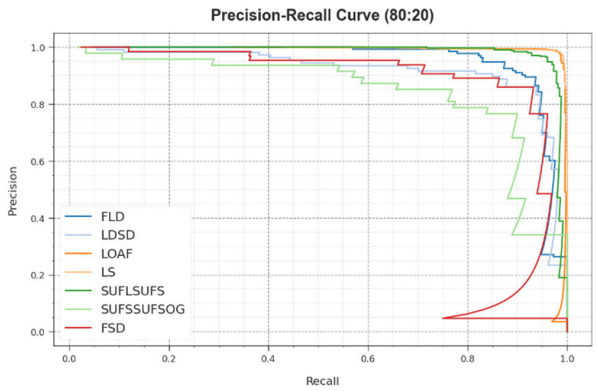

FIGURE 8. PR curve of ICOADL-HAR technique on 80:20 of TRPH/TSPH.

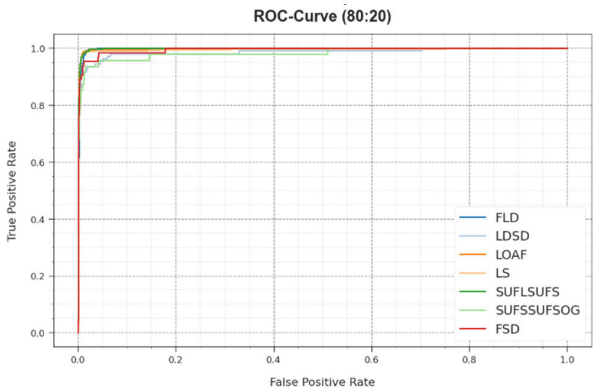

FIGURE 9. ROC curve of ICOADL-HAR technique on 80:20 of TRPH/TSPH.

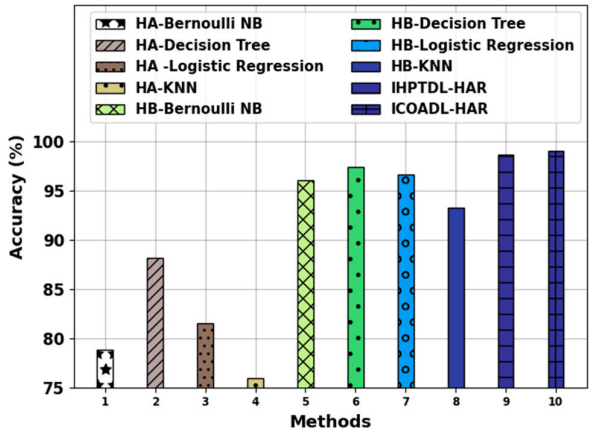

FIGURE 10. *Accu$_y$* outcome of ICOADL-HAR technique with other existing models.

TABLE 4. *Accu$_y$* outcome of ICOADL-HAR technique with other existing models.

Methods	Accuracy
HA-Bernoulli NB	78.86
HA-Decision Tree	88.17
HA -Logistic Regression	81.55
HA-KNN	75.95
HB-Bernoulli NB	96.07
HB-Decision Tree	97.38
HB-Logistic Regression	96.66
HB-KNN	93.26
IHPTDL-HAR	98.70
ICOADL-HAR	99.01

its parameters to minimize the discrepancies between the actual training and the prediction labels.

With respect to the PR curve as shown in Fig. 8, the outcomes confirm that the ICOADL-HAR technique on 80:20 of TRPH/TSPH steadily accomplishes improved PR values across every class. The results highlight the effectual capability of the model in the discrimination of various classes, highlighting the efficiency in the detection of classes.

Furthermore, in Fig. 9, we introduce ROC curves generated by the ICOADL-HAR method on 80:20 of TRPH/TSPH, which excel in distinguishing between the classes. This curve provides essential insights into the balance between TPR and FPR across various classification thresholds and epochs. The results highlight the accurate classification performance under various classes, which highlights the performance in tackling various classification problems.

In Table 4 and Fig. 10, a comprehensive comparison analysis of the ICOADL-HAR model is provided [23]. The results imply that the ICOADL-HAR technique gains better performance with an increased $accu_y$ of 99.01%. On the other hand, the HA-Bernoulli NB, HA-Decision Tree, HA -Logistic

Regression, HA-KNN, HB-Bernoulli NB, HB-Decision Tree, HB-Logistic Regression, HB-KNN, and IHPTDL-HAR models obtain worse performance with minimal $accu_y$ values of 78.86%, 88.17%, 81.55%, 75.95%, 96.07%, 97.38%, 96.66%, 93.26%, and 98.70%, correspondingly. These results ensured that the ICOADL-HAR technique accomplishes enhanced recognition results in the healthcare environment.

V. CONCLUSION

In this study, we have established an ICOADL-HAR approach for healthcare monitoring. The purpose of the ICOADL-HAR technique is to analyze the sensor information of the patients to determine the different kinds of activities. It contains three main processes such as Z-score normalization, ALSTM-based classification, and ICOA-based hyperparameter tuning. In the primary stage, the ICOADL-HAR technique allows a data normalization process using the Z-score approach. For activity recognition, the ICOADL-HAR technique employs the ALSTM model. Finally, the hyperparameter tuning of the ALSTM algorithm can be performed by using the ICOA. The stimulation validation of the ICOADL-HAR method takes place using benchmark HAR datasets. The wide-ranging comparison analysis highlighted the improved recognition rate of the ICOADL-HAR model compared to other existing HAR approaches with a maximum accuracy of 99.01%. In the future, the ICOADL-HAR technique holds significant latent for more developments in the medical sector. Exploring real-time execution and combination with evolving technologies namely edge computing improve the responsiveness and effectiveness of the healthcare monitoring system. Furthermore, extending the ICOADL-HAR methodology to varied patient populations and medical settings will contribute to its generalizability and applicability across several healthcare conditions.

ACKNOWLEDGMENT

The authors extend their appreciation to the Deanship of Scientific Research at King Khalid University for funding this work through large group Research Project under grant number (RGP2/29/44). Research Supporting Project number (RSPD2024R521), King Saud University, Riyadh, Saudi Arabia. This study is partially funded by the Future University in Egypt (FUE).

REFERENCES

[1] S. Hurtado, J. García-Nieto, A. Popov, and I. Navas-Delgado, "Human activity recognition from sensorised patient's data in healthcare: A streaming deep learning-based approach," *Int. J. Interact. Multimedia Artif. Intell.*, vol. 8, no. 1, p. 23, 2023.

[2] D. Bhattacharya, D. Sharma, W. Kim, M. F. Ijaz, and P. K. Singh, "Ensem-HAR: An ensemble deep learning model for smartphone sensor-based human activity recognition for measurement of elderly health monitoring," *Biosensors*, vol. 12, no. 6, p. 393, Jun. 2022.

[3] A.-C.-P. Patricia, V. Enrico, B. A. Shariq, E. De la Hoz Franco, P.-M.-M. Alberto, O.-C.-A. Isabel, M. I. Tariq, J. K. G. Restrepo, and P. Fulvio, "Machine learning applied to datasets of human activity recognition: Data analysis in health care," *Current Med. Imag. Rev.*, vol. 19, no. 1, pp. 46–64, Jan. 2023.

[4] E. Shalaby, N. ElShennawy, and A. Sarhan, "Utilizing deep learning models in CSI-based human activity recognition," *Neural Comput. Appl.*, vol. 34, no. 8, pp. 5993–6010, Apr. 2022.

[5] J. V. Jeyakumar, A. Sarker, L. A. Garcia, and M. Srivastava, "X-CHAR: A concept-based explainable complex human activity recognition model," *Proc. ACM Interact., Mobile, Wearable Ubiquitous Technol.*, vol. 7, no. 1, pp. 1–28, Mar. 2022.

[6] A. Snoun, T. Bouchrika, and O. Jemai, "Deep-learning-based human activity recognition for Alzheimer's patients' daily life activities assistance," *Neural Comput. Appl.*, vol. 35, no. 2, pp. 1777–1802, Jan. 2023.

[7] E. Ramanujam, T. Perumal, and S. Padmavathi, "Human activity recognition with smartphone and wearable sensors using deep learning techniques: A review," *IEEE Sensors J.*, vol. 21, no. 12, pp. 13029–13040, Jun. 2021.

[8] S. Zhang, Y. Li, S. Zhang, F. Shahabi, S. Xia, Y. Deng, and N. Alshurafa, "Deep learning in human activity recognition with wearable sensors: A review on advances," *Sensors*, vol. 22, no. 4, p. 1476, Feb. 2022.

[9] V. Soni, H. Yadav, V. B. Semwal, B. Roy, D. K. Choubey, and D. K. Mallick, "A novel smartphone-based human activity recognition using deep learning in health care," in *Machine Learning, Image Processing, Network Security and Data Sciences*. Singapore: Springer, 2021, pp. 493–503.

[10] N. Dua, S. N. Singh, S. K. Challa, V. B. Semwal, and M. L. S. S. Kumar, "A survey on human activity recognition using deep learning techniques and wearable sensor data," in *Proc. Int. Conf. Mach. Learn., Image Process., Netw. Secur. Data Sci.* Cham, Switzerland: Springer, 2022, pp. 52–71.

[11] S. An, G. Bhat, S. Gumussoy, and U. Ogras, "Transfer learning for human activity recognition using representational analysis of neural networks," *ACM Trans. Comput. Healthcare*, vol. 4, no. 1, pp. 1–21, Jan. 2023.

[12] N. T. Hoai Thu and D. S. Han, "HiHAR: A hierarchical hybrid deep learning architecture for wearable sensor-based human activity recognition," *IEEE Access*, vol. 9, pp. 145271–145281, 2021.

[13] M. A. Khatun, M. A. Yousuf, S. Ahmed, M. Z. Uddin, S. A. Alyami, S. Al-Ashhab, H. F. Akhdar, A. Khan, A. Azad, and M. A. Moni, "Deep CNN-LSTM with self-attention model for human activity recognition using wearable sensor," *IEEE J. Transl. Eng. Health Med.*, vol. 10, pp. 1–16, 2022.

[14] N. Dua, S. N. Singh, V. B. Semwal, and S. K. Challa, "Inception inspired CNN-GRU hybrid network for human activity recognition," *Multimedia Tools Appl.*, vol. 82, no. 4, pp. 5369–5403, Feb. 2023.

[15] H. Park, N. Kim, G. H. Lee, and J. K. Choi, "MultiCNN-FilterLSTM: Resource-efficient sensor-based human activity recognition in IoT applications," *Future Gener. Comput. Syst.*, vol. 139, pp. 196–209, Feb. 2023.

[16] Y.-W. Kim, K.-L. Joa, H.-Y. Jeong, and S. Lee, "Wearable IMU-based human activity recognition algorithm for clinical balance assessment using 1D-CNN and GRU ensemble model," *Sensors*, vol. 21, no. 22, p. 7628, Nov. 2021.

[17] C. Han, L. Zhang, Y. Tang, W. Huang, F. Min, and J. He, "Human activity recognition using wearable sensors by heterogeneous convolutional neural networks," *Expert Syst. Appl.*, vol. 198, Jul. 2022, Art. no. 116764.

[18] A. J. Abdulelah, M. Al-Kubaisi, and A. M. Shentaf, "An efficient human activity recognition model based on deep learning approaches," *Indonesian J. Electr. Eng. Informat.*, vol. 10, no. 1, pp. 177–186, Mar. 2022.

[19] M. A. Imron and B. Prasetyo, "Improving algorithm accuracy k-nearest neighbor using z-score normalization and particle swarm optimization to predict customer churn," *J. Soft Comput. Explor.*, vol. 1, no. 1, pp. 56–62, 2020.

[20] N. Bacanin, L. Jovanovic, M. Zivkovic, V. Kandasamy, M. Antonijevic, M. Deveci, and I. Strumberger, "Multivariate energy forecasting via metaheuristic tuned long-short term memory and gated recurrent unit neural networks," *Inf. Sci.*, vol. 642, Sep. 2023, Art. no. 119122.

[21] X. Lei, D. Shilin, T. Shangqin, H. Changqiang, D. Kangsheng, and Z. Zhuoran, "Beyond visual range maneuver intention recognition based on attention enhanced tuna swarm optimization parallel BiGRU," *Complex Intell. Syst.*, vol. 2023, pp. 1–22, Oct. 2023.

[22] M. Kong, X. Gou, and G. Fathi, "Enhancing energy efficiency in rural CCHP systems with optimal gas engine size selection and improved coyote optimizer," *Energy Rep.*, vol. 10, pp. 3146–3157, Nov. 2023.

[23] E. Dhiravidachelvi, M. S. Kumar, L. D. Vijay Anand, D. Pritima, S. Kadry, B.-G. Kang, and Y. Nam, "Intelligent deep learning enabled human activity recognition for improved medical services," *Comput. Syst. Sci. Eng.*, vol. 44, no. 2, pp. 961–977, 2023.